Corrosion Properties of Inconel 617 Alloy after Heat Treatment at Elevated Temperature

A. Kewther, B.S. Yilbas, and M.S.J. Hashmi

(Submitted 27 July 2000)

Inconel alloys find wide application in industry as high-temperature resistance materials. In the present study, refurbishment of the Inconel 617 alloy after 37,000 h of operation in the field is carried out through the heat-treatment process. The electrochemical response of the heat-treated alloy is determined through potentiodynamic testing of the surfaces. The heat-treatment process is carried out at 1175 °C for 1 and 2 h in an air free furnace. The corrosion rate is estimated from TAFEL and polarization measurements. The surface morphology after the electrochemical tests is studied using scanning electron microscopy (SEM), while the material characterization at the surface is carried out using energy disperse spectroscopy (EDS). It is found that the corrosion resistance improves considerably for the workpieces subjected to 1 h heat treatment. The depletion of Cr and Mo at grain boundaries results in excessive pitting in this region. Moreover, enrichment of Cr at the surface after 1 h heat treatment reduces the corrosion current.

Keywords 37,000 h of service, electrochemical tests, heat treatment, Inconel 617, long-term exposure

1. Introduction

Inconel (EG&G, USA) alloys have been widely used as high-temperature materials in pressure vessels and hot path components of gas turbine engines. The Inconel 617 alloy is a solid solution nickel-based alloy, which contains chromium, cobalt, molybdenum, and aluminum. The aluminum and chromium contents protect the alloy from oxidation reactions at high temperature. This feature enables the alloy to be used as hot path components in gas turbine engines. As the hot path component is used over 37,000 h of operation in a gas turbine engine, the material properties degragate and refurbishment of the alloy becomes essential for further usage. One of the methods for the refurbishment process is the heat treatment of the alloy.[1] The surface properties of the alloy change slightly after the heat-treatment process. This requires the examination of the surface properties of the alloy after the heat-treatment process.

Considerable research studies were carried out to examine the metallurgical and mechanical properties of the alloy at elevated temperatures. The heat treatment of the Inconel 617 alloy was investigated previously.[2] It was indicated that the tensile properties of the alloy improved, while the fatigue resistance did not alter after the heat-treatment process. Venkatesh and Rack[3] investigated the strain hardening of the Inconel 690 alloy during tensile deformation at temperatures between 200 and 1200 °C. They indicated that the third stage of hardening in the Inconel alloy at temperatures between 600 and 700 °C and single stage hardening between 750 and 1200 °C could be described by the Bodner-Partom and/or Kock-Mecking dislocation-dislocation interaction model. The microstructures and mechanical properties of laser-welded Inconel alloy were investigated by Hirose *et al.*[4] They observed an interdentritic gamma phase in the fusion zone of the laser-welded samples. The effect of gamma prime depletion on the creep behavior after high-temperature treatment of the Inconel alloy was investigated by Pandey and Satyanarayana.[5] They showed that gamma prime depletion in the air-exposed samples caused a weakening effect, leading to enhanced creep rate. High-temperature creep and tensile properties of the Inconel alloy were examined by Chavaz *et al.*[6] They developed data for the creep and tensile properties of the alloy at elevated temperatures. The etching properties of the Inconel alloy due to low-cycle fatigue at high temperatures were investigated by Komazaki *et al.*[7] A chemical etching technique was used to detect the fatigue damage. They showed that the density of slip bands increased with increased fatigue life and demonstrated the applicability of the etching technique to fatigue damage evaluation.

Considerable research studies were carried out to examine the corrosion properties of Inconel alloys. The pitting corrosion of the mill-annealed Inconel 600 alloy in chloride and thiosulfate anion solutions at low temperature was investigated by Ho and Yu.[8] They indicated that sulfur was enriched in pits in the processing of pit growth. In addition, they observed that pit density and average pit depth increased with increasing concentrations of sodium chloride and temperature of solution. Seawater corrosion behavior of the laser-processed Inconel alloy was investigated by Cooper *et al.*[9] They modified the surfaces by a laser assisting particle injection. The modification techniques include laser melting and laser assisting WC and TiC injections. They showed that corrosive damage was more severe in the WC-injected sample than in the TiC-injected and laser-melted samples. Moreover, they indicated that, to minimize seawater corrosion by laser-modified surfaces, the microstructures had to be homogenized and dissolution and alloying had to be avoided while adding particulate material. The effect of structural evolution in the Inconel alloy on intergranular corrosion

A. Kewther and **M.S.J. Hashmi,** Mechanical and Manufacturing Engineering Department, Dublin City University, Dublin, Ireland; and **B.S. Yilbas,** Mechanical Engineering Department, King Fahd University of Petroleum and Minerals, Dhahran - 31261, Saudi Arabia. Contact e-mail: bsyilbas@kfupm.edu.sa.

Table 1 Elemental composition of the Inconel 617 alloy

Ni	Cr	Co	Mo	Al	C	Fe	Mn	Si	S	Ti	Cu
Balance	22	12.5	9	1.2	0.07	1.5	0.5	0.5	0.008	0.3	0.2

Table 2 Heat-treatment conditions

Temperature (°C)	1175	1775
Duration (h)	1	2

was studied by Ganzalez-Rodrigues and Fionova.[10] They showed that a correlation existed between the intensity of intergranular corrosion of the alloy and the effect of fragmentation of large grains.

In the present study, refurbishment of the Inconel 617 alloy, which was used for 37,000 h of operation in a gas turbine engine, is investigated. A heat treatment of the alloy at elevated temperature is considered for the refurbishing process. The electrochemical response of the heat-treated surface is investigated through potentiodynamic polarization measurements in deaerated 1 N H_2SO_4 and 0.05 M NaCl aqueous solution at 25 °C.

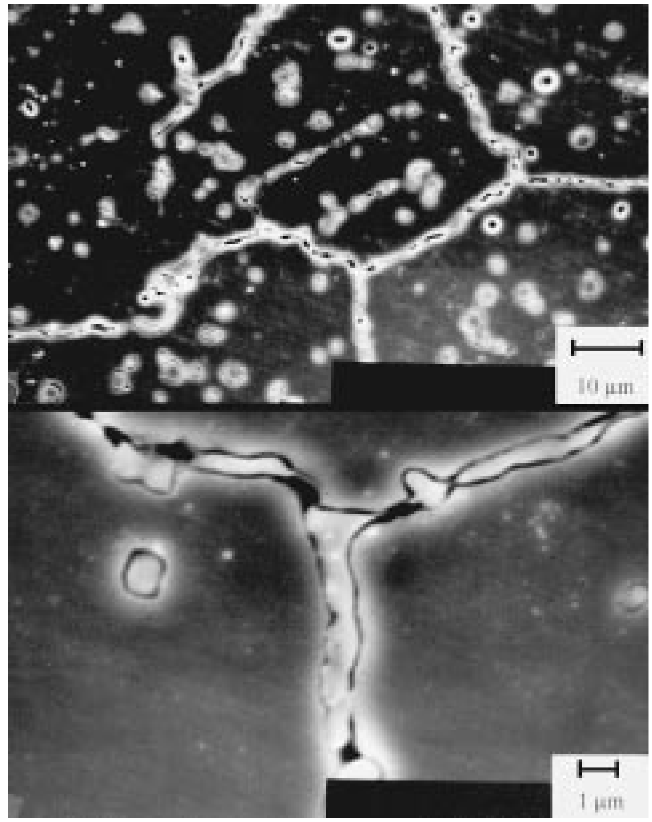

Fig. 1 Microstructure of Inconel 617 as received after 37,000 h of operation

2. Experimental

The workpiece elemental composition is given in Table 1. The workpieces were prepared from the transition piece of a gas turbine engine. The transition piece had 37,000 h of operation in the field. The workpieces were cut to 20×20 mm^2 size and ground down to 2 mm thickness. The workpieces were cleaned ultrasonically before the heat-treatment process. The high-temperature furnace was used during the heat-treatment process, and high-temperature oxidation of workpieces was prevented through replacing them in quartz tubes in the furnace. Table 2 gives the heat-treatment conditions.

A three-electrode cell was used for the electrochemical test. The cell accommodated an inlet and an outlet for an inert gas and a thermometer. A potentiostat maintaining the electrode potential within 1 mV of a preset value over a wide range of applied currents was employed. The potentiostat had a potential range of 0.6 to 1.6 V and anodic current output from 1 to 10^5 μA. A computer-controlled scanning potentiostat (EG&G model 273, United Kingdom) was used for potentiodynamic measurements. For each measurement, the potentiostat automatically varied the potential at a constant rate between two preset potentials. A record of the current and potential was plotted continuously using an *x*, *y* recorder.

During the measurements, standard methods were used: a saturated calomel electrode with controlled rate of leakage was employed as a reference electrode, and the electrolyte was an aerated 0.1 N H_2SO_4 and 0.05 M NaCl held at 25 °C. The testpieces were masked to expose a surface area of 1 cm^2.

Scanning electron microscopy (SEM) microphotography was carried out to observe the pits formed at the workpiece surfaces, while energy dispersive spectroscopy (EDS) was introduced for material characterization before and after the potentiodynamic tests.

3. Results and Discussions

The Inconel 617 alloy after 37,000 h of operation in the gas turbine engine is heat treated at 1175 °C. The electrochemical response of the heat-treated and untreated workpiece surfaces was obtained through potentiodynamic polarization measurements. The surface morphology of the workpieces after the electrochemical tests is examined using SEM.

Figure 1 shows the cross section of the workpieces before the heat-treatment process. The cavitation along the grain boundy is observed for the untreated workpiece surface; in which case, agglomeration of grain boundary carbides occurs. The multiple discontinuous creep cracks are also seen. The cavitation at the grain boundary reduces partially after the heat-treatment process. The EDS data (Table 3) reveals that the chromium content improves and aluminum degradation slows at grain boundaries after the heat-treatment process.

The potentiodynamic polarization curves for untreated and heat-treated workpieces in 0.1 N H_2SO_4 and 0.005 M NaCl aqueous solution are shown in Fig. 2. The corrosion potential for 1 h heat-treated workpiece is 132 mV, which is nobler than

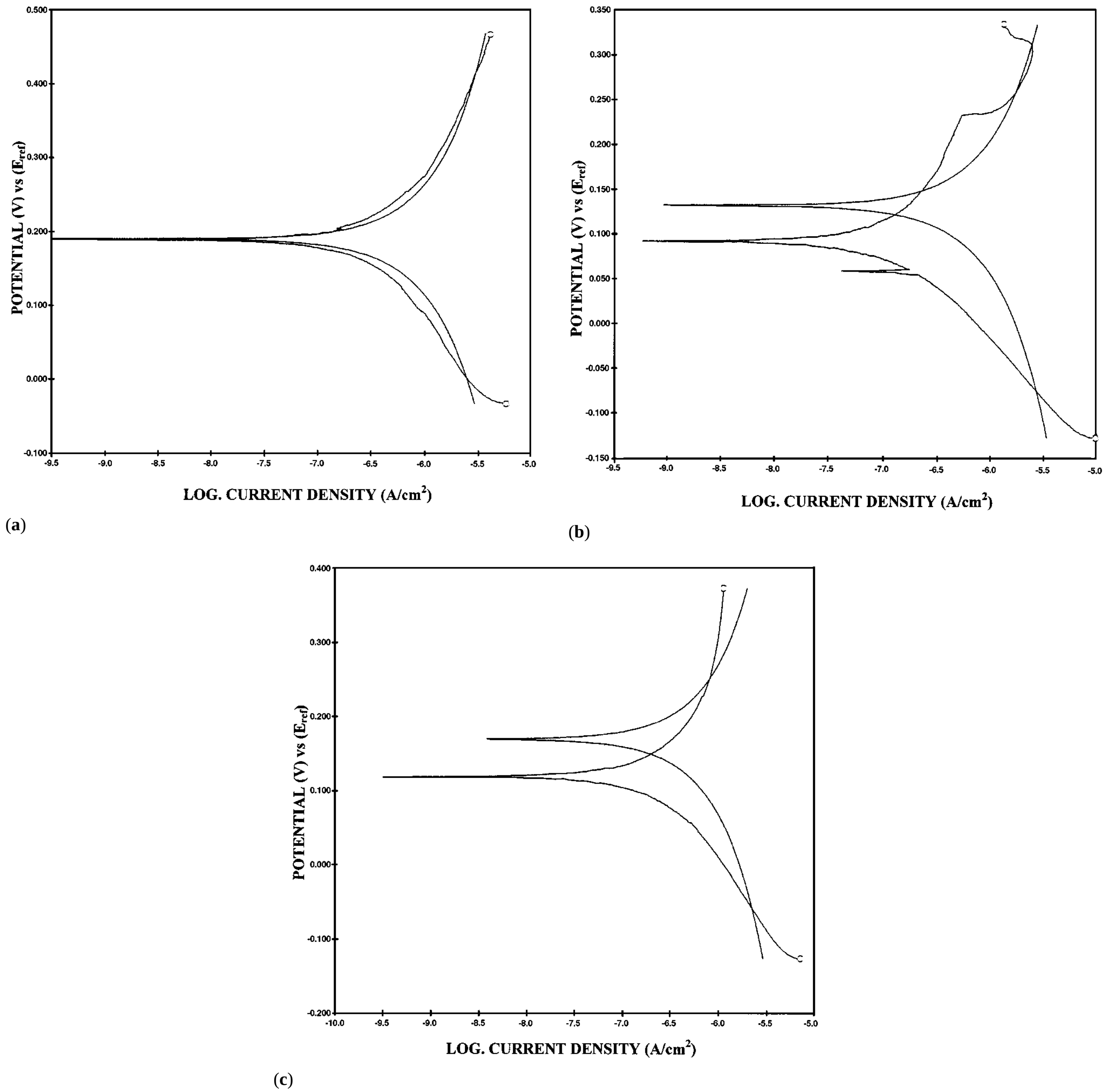

Fig. 2 (**a**) Polarization curve for untreated workpiece. (**b**) Polarization curve for 1 h heat-treated workpiece. (**c**) Polarization curve for 2 h heat-treated workpiece

Table 3 EDS results at the grain boundary of the workpieces

Variables	Al	S	Ti	V	Cr	Fe	Ni
Grain boundary as received	0.91	7.86	…	0.04	17.37	21.08	52.74
Grain boundary after 1 h heat treatment	0.01	4.63	…	0.15	22.04	21.29	51.88
Grain boundary after 2 h heat treatment	2.46	3.48	0.27	0.3	21.7	7.09	64.7

that of the untreated workpiece (190 mV). In addition, the corrosion current density for 1 h heat-treated workpiece is almost half that corresponding to the untreated surface. As the heat-treatment duration is extended to 2 h, the corrosion potential becomes higher than its counterpart corresponding to 1 h heat treatment, but it is less than that of the untreated workpiece.

Table 4 TAFEL analysis results

Variables	E_{corr} (mV)	I_{corr} ($A/cm^2 \times 10^{-7}$)	Corrosion rate (mpy)
Untreated	189.2	6.947	0.272
1 h heat treatment	92.8	1.409	0.55
2 h heat treatment	118.6	5.691	0.223

These results indicate that the heat treatment reduces the anodic dissolution of the alloy either by forming an oxide layer at the material surface or by slowing down the removal of metal ions *via* complex ion formation.

The TAFEL and polarization resistance results are given in Tables 4 and 5. A 1 h heat-treated workpiece results in a minimum corrosion rate followed by a 2 h heat-treated workpiece, and an untreated workpiece, in increasing order. The high corrosion rate of the untreated workpiece is due to the partitioning out of solution of useful alloying elements after several thousands of hours of operation. In this case, Cr, the primary alloying element, depletes in the surface region of the workpiece; *i.e.*, the protection of the external surface of the alloy by forming Cr_2O_3 is suppressed, which is the primary reason for resistance to corrosion. Moreover, the workpiece before the heat treatment has a segregated microstructure. This indicates that the material is no longer homogeneous at it was in new condition. The partitioned alloying elements combine with the residual carbon and form carbides. Once the alloying elements such as Cr and Mo form carbides, the grain boundary regions are depleted of these elements, removing their passivation protection locally.

Figure 3 to 5 show SEM microphotographs of workpiece surfaces after the electrochemical tests. The pit morphology gives the qualitative analysis of the corrosion product. The corrosion products in pits are being enriched in Cr and depleted in Ni and Fe. No specific pattern on the pit geometry is observed for the workpiece surfaces subjected to 1 h heat treatment (Fig. 4). In addition, the pit size is small and the pit density is less than the other workpieces. This indicates that a higher Cr content in the alloy increases the acidification reaction in the pit and decreases the amount of precipitation. In this case, the mouth of the pit serves as a cathode for the reduction of O_2, and it attains a noble potential. In the case of the untreated workpiece, the pit geometry shows significant lateral growth along the surface, leading to elongated pits. The pit growth saturates after some time. This implies that the reactivation of pits being passivated, *i.e.*, the secondary micropits, plays an important role in the reactivation process. Moreover, severe pitting over the grain boundary is evident from Fig. 3, in which case the formation of Cr and Mo oxides is unlikely in this region. In the case of the 2 h heat-treated workpiece (Fig. 5), localized deep pits are formed. In this case, during the pit growth, the pit bottom acts as an anode galvanically coupled to the external cathodic area, leading to a steeper potential gradient in the pit. Consequently, the pit depth increases. In the later stage, ohmic resistance to current flow inside the pit is bound to develop due to formation of insoluble pit corrosion products, causing polarization to a more noble potential and a lower corrosion current.

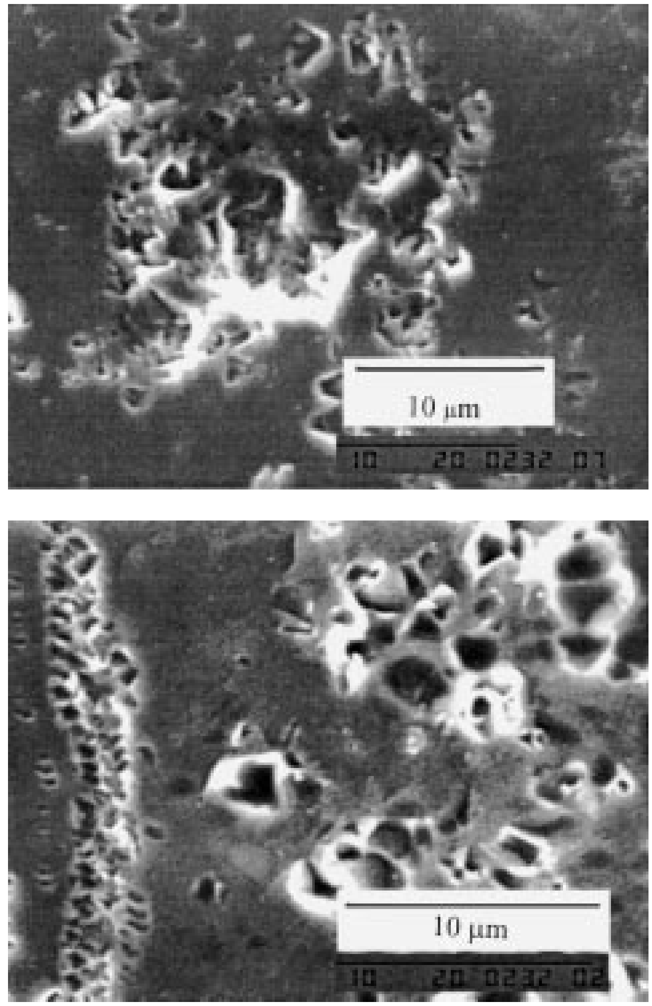

Fig. 3 SEM microphotographs of pits developed on the surface of the untreated workpiece

4. Conclusions

The heat treatment of the Inconel 617 alloy used over 37,000 h of operation in the field is studied. The electrochemical response of the untreated and heat-treated workpiece surfaces is estimated through potentiodynamic measurements. It is found that the corrosion rate measured from TAFEL and polarization tests reduces for heat-treated workpieces. The depletion of Cr at the grain boundary increases the pitting density in this region. The specific conclusions derived from the present study can be listed as follows.

- The cavitation along the grain boundaries is observed for the untreated workpieces. This reduces partially after the heat-treatment process. The multiple discontinuous creep cracks are also observed. The depletion in Cr and Al contents at the grain boundary occurs for the untreated workpieces.
- The corrosion potential and the corrosion current reveal that the heat treatment reduces the anodic dissolution of the alloy either by forming an oxide layer at the material

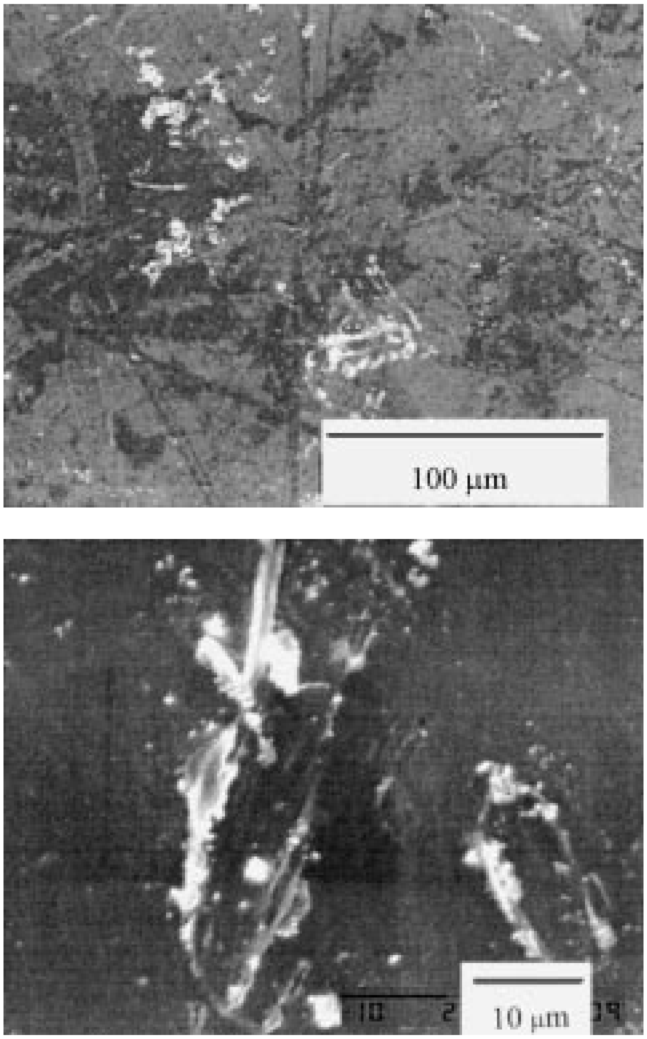

Fig. 4 SEM microphotographs of pits developed at the surface of a 1 h heat-treated workpiece

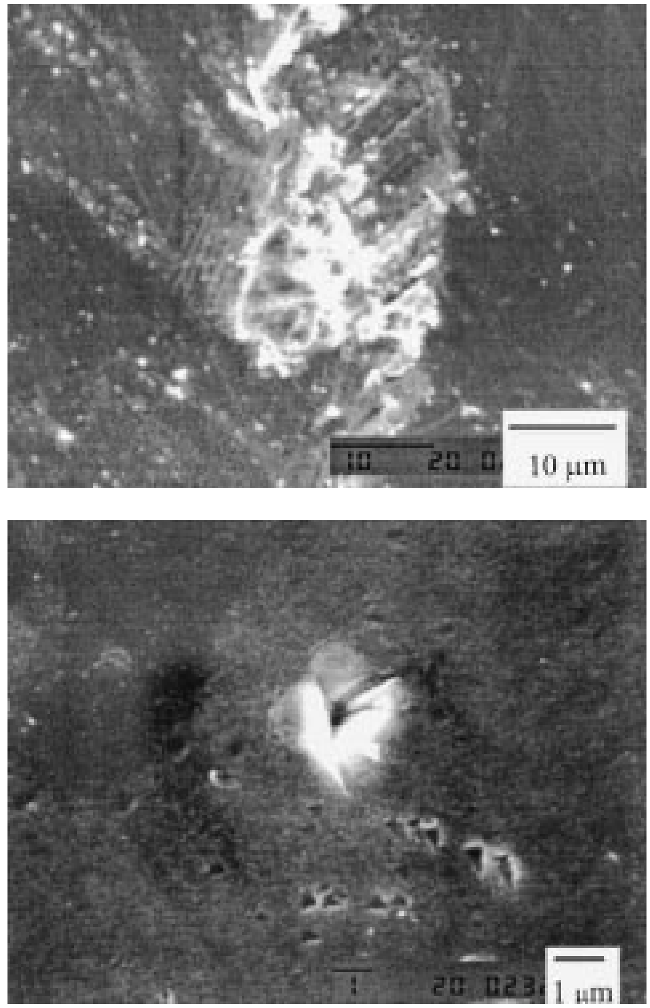

Fig. 5 SEM microphotographs of pits developed at the surface of a 2 h heat-treated workpiece

Table 5 Polarization resistance results

Variables	E_{corr} (mV)	I_{corr} (A/cm^2 $\times$ 10^{-7})	Polarization resistance (Ω/cm^2 $\times$ 10^4)	Corrosion rate (mpy)
Untreated	190.4	9.575	7.47	0.375
1 h heat treatment	132.9	4.484	7.57	0.175
1 h heat treatment	168.8	8.128	10.25	0.318

surface or by slowing down the removal of metal ions via complex ion formation.

- A 1 h heat-treated workpiece results in a minimum corrosion rate and an untreated workpiece, in increasing order. This is mainly because (1) of the partitioning out of solutions of alloying elements in the untreated workpiece after several thousand hours of operation and (2) the microstructure of the workpiece used for long hours is segregated, which, in turn, results in a nonhomogenous structure. Moreover, the alloying elements such as Cr and Mo form carbides at the grain boundary for the untreated workpiece; in which case, the passivation protection of these elements becomes less in this region.
- The pit geometry does not yield any specific pattern. The pit size is small and its density is low for a 1 h heat-treated workpiece. In general, the shallow pits are observed at the

workpiece surfaces. This suggests that the ohmic resistance to current flow inside the pit is bound to develop due to formation of insoluble pit corrosion products, which cause polarization to a more noble potential and a lower corrosion current.

Acknowledgments

Acknowledgments are due to the King Fahd University of Petroleum and Minerals and Dublin City University.

References

1. V.P. Swaminathan, H.B. Owens, and N. Hicks: *Proc. Int. Gas Turbine and Aeroengine Congr. and Exp.*, Cologne, Germany, June 1–4, 1992.
2. M. Kewther-Ali, M.S.J. Hashmi, and B.S. Yilbas: *Proc. Int. Conf. on Advances in Materials and Processing Technologies*, AMPT '99, Ireland, Aug. 3–6, 1999, Dublin City University, Ireland, 1999, pp. 963-69.
3. V. Venkatesh and H.J. Rack: *Mech. Mater.*, 1998, vol. 30, pp. 69-81.
4. A. Hirose, K. Sakata, and K.F. Kobayashi: *Int. J. Mater. Product Technol.*, 1998, vol. 13, pp. 28-44.
5. M.C. Pandey and D.V.V. Satyanarayana: *Bull. Mater. Sci.*, 1996, vol. 19, pp. 1009-15.
6. S.A. Chavez, G.E. Korth, D.M. Harper, and T.J. Walker: *Nucl. Eng. Design*, 1994, vol. 148, pp. 351-63.
7. S. Komazaki, Y. Watanabe, and T. Shoji: *Trans. Jpn. Soc. Mech. Eng.*, 1997, Part A, vol. 63A, pp. 1481-88.
8. J.T. Ho and G.P. Yu: *Corrosion*, 1992, vol. 48, pp. 147-58.
9. K.P. Cooper, P. Slabodnick, and E.D. Thomas: *Mater. Sci. Eng. A: Struct. Mater., Microstr. and Processing*, 1996, vol. A206, pp. 138-49.
10. J.G. Gonzalez-Rodriguez and L. Fionova: *Mater. Chem. Phys.*, 1998, vol. 56, pp. 70-73.